Pacific Northwest
NATIONAL LABORATORY

PNNL-33610

A Review: PFAS Adsorption, Sensing, and Remediation with Engineered Nanoporous Materials

October 2022

Radha Kishan Motkuri
Julian Schmid
Dushyant Barpaga
Yu H. Cheng
Gabriel Hall
Vaithiyalingam Shutthanandan
Sayandev Chatterjee
Sagnik Basuray
Pete McGrail

U.S. DEPARTMENT OF ENERGY

Prepared for the U.S. Department of Energy
under Contract DE-AC05-76RL01830

DISCLAIMER

PACIFIC NORTHWEST NATIONAL LABORATORY
operated by
BATTELLE
for the
UNITED STATES DEPARTMENT OF ENERGY
under Contract DE-AC05-76RL01830

Printed in the United States of America

Available to DOE and DOE contractors from the Office of Scientific and Technical Information,
P.O. Box 62, Oak Ridge, TN 37831-0062
www.osti.gov
ph: (865) 576-8401
fax: (865) 576-5728
email: reports@osti.gov

Available to the public from the National Technical Information Service
5301 Shawnee Rd., Alexandria, VA 22312
ph: (800) 553-NTIS (6847)
or (703) 605-6000
email: info@ntis.gov
Online ordering: http://www.ntis.gov

PNNL-33610

A Review: PFAS Adsorption, Sensing, and Remediation with Engineered Nanoporous Materials

October 2022

Radha Kishan Motkuri
Julian Schmid
Dushyant Barpaga
Yu H. Cheng
Gabriel Hall
Vaithiyalingam Shutthanandan
Sayandev Chatterjee
Sagnik Basuray
Pete McGrail

Prepared for
the U.S. Department of Energy
under Contract DE-AC05-76RL01830

Pacific Northwest National Laboratory
Richland, Washington 99354

Abstract

Per- and polyfluoroalkyl substances (PFAS) are among the most abundant environmental contaminant species. They are widespread due to uncontrolled industrial and commercial use and have been linked to health risks such as cancer. With rising global concerns about the public health effects of PFAS, there is an incentive to develop strategies for reliable monitoring and effective PFAS removal, particularly in drinking water. Traditional PFAS sensing techniques are inefficient due to long measurement times, high labor input, high costs, and limitations to ex situ analysis. Current commercially available sorbents for PFAS removal generally lack the ability to capture PFAS components rapidly and quantitatively. Furthermore, existing sorbents are notably inefficient in removing the more toxic, smaller PFAS chemical chains. Large-scale applications of these methods tend to be costly and resource-intensive. Pacific Northwest National Laboratory has developed unique strategies for PFAS sensing and removal with capture probe technology that has an affinity for fluorocarbons, including PFAS. For both sensing and removal, the customizable capture probes can target specific PFAS compounds since they used a metal-organic framework (MOF)-based technology that can be fine-tuned and molecularly tailored. This tailoring of the materials enables high PFAS sensitivity, selectivity, and faster uptake. PNNL's capture probe materials have been developed into a sensing technique based on the interactions of the capture probes with PFAS at the molecular level and further transduced that to a quantifiable electrochemical response. The materials have been integrated into a sensor platform developed by New Jersey Institute of Technology (NJIT). Tunable capture probes with a range of detection sensitivities allow for faster and more sensitive PFAS detection limits as low as what appears to be 0.5 ng/L (compared to the U.S. Environmental Protection Agency health advisory level of 70 ng/L). Customization of the capture probe results in improved sorption capacities (fast kinetics and high capacities) compared to commercial granular activated carbons. This research applied various experimental and modeling tools to improve understanding the molecular level interactions between the sorbents towards PFAS adsorption properties.

Acknowledgments

The research described in this report was conducted under the Laboratory Directed Research and Development (LDRD) Program as a strategic investment at the Pacific Northwest National Laboratory (PNNL), a multiprogram national laboratory operated by Battelle for the U.S. Department of Energy. PNNL is a multi-program national laboratory operated for the U.S. Department of Energy (DOE) by Battelle Memorial Institute under Contract No. DE-AC05-76RL01830.

Contents

Figures

Tables

1.0 Introduction

Per- and polyfluoroalkyl substances (PFAS) are a group of over 5000 human-made compounds that consist of a hydrophobic, fluorine-saturated carbon chain, and a hydrophilic functional group (Fig. 1). Many PFAS are resistant to grease, oil, water, and heat, which makes them suitable to be used in a range of applications, such as stain- and water-resistant fabrics and carpeting, cleaning products, paints, and fire-fighting foams. Some PFAS are authorized by the U.S. Food and Drug Administration for limited use in cookware, food packaging, and food processing equipment. Widespread use of these materials coupled with their stability against degradation under the influence of the environment has led to an accumulation of considerable amounts of PFAS in air, soil, and water. This PFAS accumulation is believed to pose a greater risk to human health, compelling the U.S. Environmental Protection Agency (EPA) to establish the health advisory levels for perfluorooctanesulfonate (PFOS) and its carboxylic acid analog PFOA in drinking water at 70 parts per trillion [1-3].

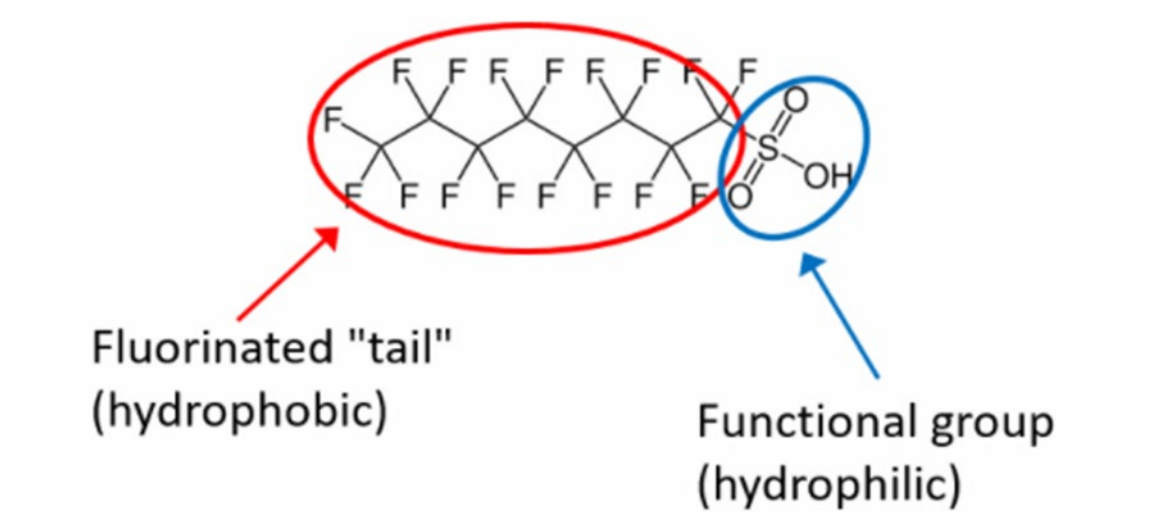

Fig. 1. PFOS structure with hydrophobic carbon chain and hydrophilic sulfonated acid group as exemplary representation of PFAS compounds [1].

Remediation strategies to address this challenge include sensing, capturing, and destruction of PFAS contaminations in drinking water. Conventional approaches to remediate PFAS, like air stripping, thermal treatment, soil vapor extraction, and hydroxyl-based chemical oxidation, have been shown to be ineffective in treating PFAS. A more promising approach that has already found an application for PFAS remediation and is worth investigating further are sorption-based removal techniques. The most widely applied material that has been used as an adsorbent for this purpose is activated carbon. While granular activated carbon (GAC) has shown to remove PFOS from groundwater with good efficiency, it was not as efficient in removing shorter chain PFAS due to slower sorption kinetics and suffered from very low sorption capacities. New emerging sorbents need to be tailored to exhibit high affinity and quick adsorption kinetics toward shorter chain PFAS like perfluorobutyrate (PFBA) and perfluorobutane sulfonic acid ate (PFBS) in order to fill that gap [4-8].

In this direction, our efforts have focused on developing novel adsorbent materials that have a high affinity toward the desired PFAS compound paired with rapid sorption kinetics. Over the past

decade, Pacific Northwest National Laboratory (PNNL) has generated numerous nanoporous materials for the capture of various fluorocarbons, including C1 to C4 fluorocarbons. Our fluorocarbon adsorption studies have included covalent organic frameworks (COFs), zeolites, hierarchical porous carbons (HPCs) and, metal-organic frameworks (MOFs) as sorbent materials (Fig. 2) [9-11]. Using in situ experiments and molecular modeling studies, we observed positive affinities between fluorine groups and the metal center of MOFs [12-15]. More importantly, the knowledge of the exact interactions of the PFAS with the properties of the MOFs provides the opportunity to reveal the mechanism of fluorocarbon adsorption. This information can be used to design future sorbent materials for applications in a fluorine-containing materials, including PFAS.

By fine-tuning the MOF material, we were able to develop materials that showed improved selectivity, sensitivity, and capacity for PFAS adsorption compared to sorbents currently used by U.S. government agencies, such as the Department of Energy (DOE), the Department of Defense (DoD), and the EPA. Tailoring these materials to target PFAS in environmental water sources is a promising approach to further improving material performance. One of our methods was to equip the nanopores of the sorbent materials with appropriate surface functionalities or metal centers. This enhances the interaction between PFAS and the sorbent or the overall treatment particle porosity to achieve higher effectivity of PFAS adsorption. This is important because the affinity between PFAS molecules and the sorbent is maintained even with interferences from highly concentrated impurities, which are ubiquitous in real-world applications.

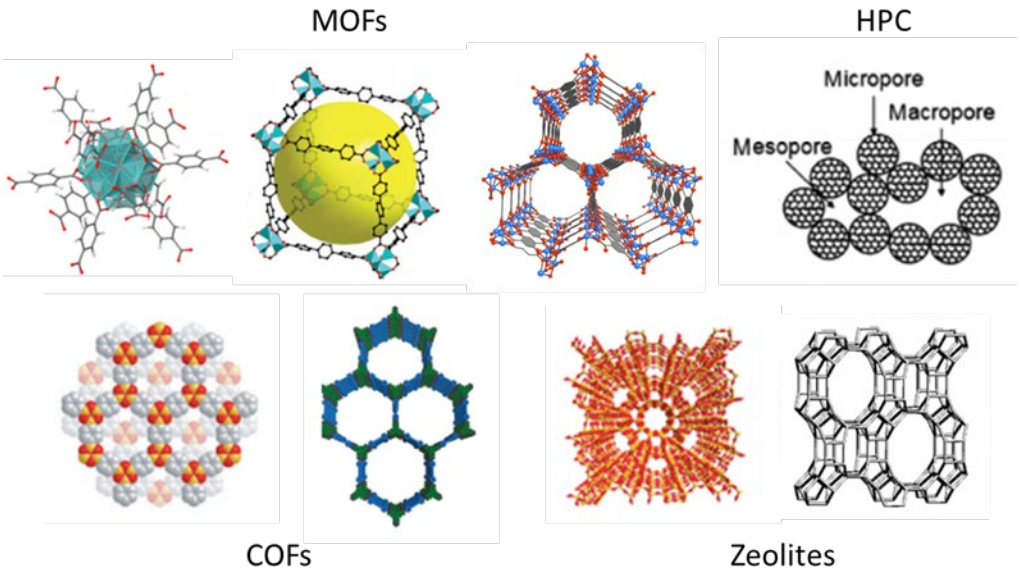

Fig. 2. Examples of nanoporous materials including MOFs, COFs, HPCs and zeolites [16-22].

2.0 Discussion

2.1 Capture probes for targeted PFAS adsorption

The pores of the materials such as MOFs, COFs, zeolites, and HPCs were engineered in order to optimize criteria like the surface area and super fluorophilicity of the functional groups or the metal centers. Furthermore, due to the large ratio of water in the samples, the stability of the materials under aqueous conditions must be accounted for. The uptake of various PFAS compounds with different end groups and fluorocarbon chain lengths was tested with solutions of the respective PFAS in deionized water and groundwater. The groundwater used in these studies was obtained from DOE well 299-W19-36 at the Hanford Site (TABLE I).Solutions of the different concentrations of PFAS were combined with a defined amount of porous materials for a specific amount of time (~300 h). The initial concentration as well as the concentration of the solutions after the contact procedure were measured by 19F nuclear magnetic resonance (NMR). Generally, the materials made for targeted PFAS uptake showed higher adsorption capacity compared to materials employed by DoD (e.g. GAC and weak anion exchangers) due to optimized porosity and sorbent sorbate interactions of the capture probes and the respective PFAS [10, 11, 13, 23, 24].

Table I. Composition of groundwater from DOE well 299-W19-36 at Hanford, WA

Constituent	**µg/L**	**Constituent**	**µg/L**
Calcium	122,000	Nitrate	317,000
Chloride	181,000	Sodium	118,000
Total Cr	17.3	Potassium	7,010
Cr(VI)	0.05	Carbonate	116,000
Magnesium	36,400	Organics	123,000

The influence of the metal center in MOFs on the efficiency of a sorbent-sorbate system is exemplified using PFOS adsorption on two different MOFs, namely Fe-MIL 101 and Cr-MIL 101 materials. [11,13]. For that purpose, ~8 mg of both materials were exposed to 800 μL of 10 mM PFOS solutions in water. The PFOS concentration in the supernatant solution after exposure was quantified by 19F -NMR spectroscopy using the peak at ~79 ppm. The decrease in peak intensity after a long exposure of the materials to the solution was attributed to the continuous disappearance of PFOS from the bulk phase of the supernatant (Fig. 3).

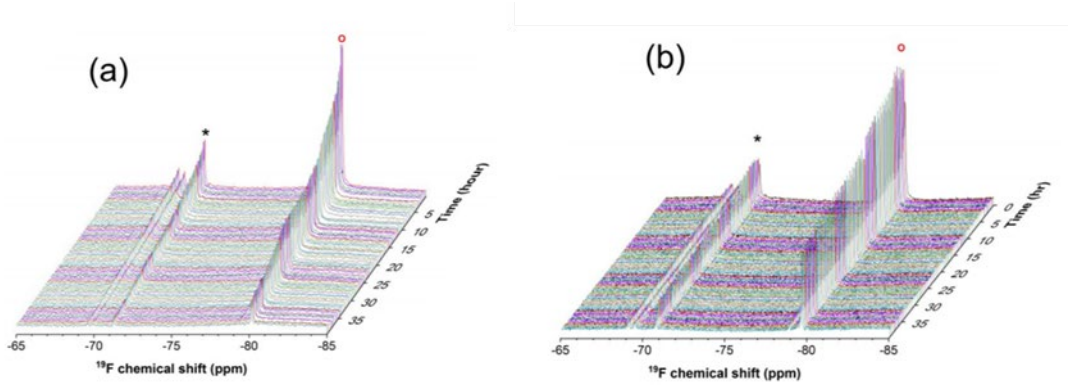

Fig. 3. ^{19}F NMR results obtained from 10 mM PFOS/H_2O mixed with (a) CrMIL-101 (8.6 mg); (b) Fe-MIL-101 (8.2 mg) after time of exposition at room temperature (~25 °C) [9].

These in situ NMR experiments show that both the Fe-MIL-101 and Cr-MIL 101 were able to adsorb and immobilize PFOS from the stock solutions. A closer look at our data reveals that PFOS concentration in the bulk solution decreased rapidly in the first minutes of exposure (~30 min) and slowly reach a plateau after longer sorption times (~40 h) (Fig. 4). Fitting the intensity profiles after sorption for the materials with a double exponential decay (Eq. 1) gave further quantitative insight into the performance of the PFOS capturing process.

$$y = A_1 e^{\frac{-t}{\tau_1}} + A_2 e^{\frac{-t}{\tau_2}} \qquad \text{(Eq. 1)}$$

A_1 and A_2 represent fit constants, while τ_1 and τ_2 are time constants. Comparison of the fitting results (TABLE II) indicates that PFOS sorption on Cr-MIL-101 was accelerated by a factor of 2 versus Fe-MIL-101. Extrapolating the fit to higher time values shows that the plateau indicating the maximum possible removal of PFOS from the bulk phase of the supernatant is reached at ~250 h on Fe-MIL-101, while it only takes ~125 h to reach the plateau on Cr-MIL-101. We assigned these differences in performance to the higher affinity of the Cr center to both S and F, while the Fe center presumably shows a higher affinity towards softer Lewis bases like the carboxylic acid analog PFOA [9].

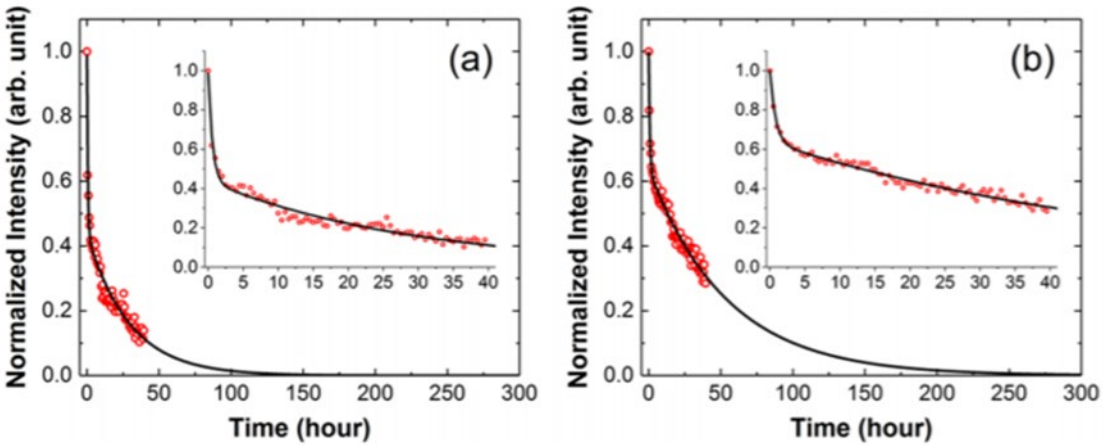

Fig. 4. Normalized peak areas of the 19F NMR peak centered at ~79 ppm (O) monitored after different sorption times after addition of 800 µL of 10 mM PFOS/H2O to (a) Cr-MIL-101 (8.6 mg) and (b) Fe-MIL-101 (8.2 mg). Red circles represent collected data while black lines represent fitted curves. Insets show data and corresponding fits for the first 40 h of data collection [9].

We performed X-ray photoelectron spectroscopy (XPS) studies on Cr-MIL-101 and Fe-MIL-101 before and after exposure to PFOS to gain further insight into the PFOS capture mechanism. We observe that the Cr p3/2 region of the pristine Cr-MIL-101 sample resolves into two species at binding energies of 577.1 and 578.2 eV, respectively, with the main contribution coming from the lower oxidation state. After exposure of Cr-MIL-101 to PFOS, the X-ray photoelectron spectra showed an increase in intensity for the higher oxidation state, indicating that Cr is oxidized during exposure to PFOS. A similar, yet smaller change of intensity occurred in the Fe p3/2 region of Fe-MIL-101 shifting the binding energy maxima from 711.8 eV in the pristine sample to 712.1 eV in the sample that was exposed to PFOS. That observation suggests that the sorption affinity of PFOS is larger for Cr than it is for Fe. Unsurprisingly, the opposite shift was apparent in the F region of the XPS spectra for unexposed PFOS, which showed a single, 1 s line at 689.3 eV vs. PFOS that was brought to contact with the MOFs exhibiting a second F environment with lower binding energy at 688.5 eV, indicating a reduction of the F center.

Comparing the fluorine spectra for the two PFOS-exposed MOFs shows that the fluorine atoms in PFOS that were contacted with Fe-MIL-101 have a more reduced environment than PFOS in Cr-MIL-101, pointing at a stronger interaction of the hydrophobic fluorinated PFOS tail with Fe. On the other hand, the S region of the photoelectron spectra indicates a stronger interaction of PFOS with Cr as the 2p3/2 sulfur line is shifting from 169.5 eV for the fresh PFOS sample to 168.3 eV for the sample that was sorbed onto Cr-MIL-101 and 168.8 eV for the sample that was sorbed onto Fe-MIL-101, respectively. Because the PFOS concentrations in our samples exceeded the critical micelle concentration, suggesting that there are more sulfur-containing moieties exposed to adsorption sites, we give more importance to the S spectra compared to the F spectra for the analysis of the binding affinities of PFOS to the two MOFs. This assumption is supported by the larger change of the intensity shift in the S region of the spectra compared to the F region. Conclusively, because of the above-mentioned points we propose that Cr metal is able to bind the majorly exposed sulfonate groups in PFOS stronger than Fe-MIL-101, leading to higher overall interaction for this host-guest-system [9].

Table II. Fit parameters and coefficients of determination from the double exponential decay equation using ^{19}F liquid phase NMR data for PFOS sorption on Cr-MIL-101 and Fe-MIL-101 [9].

	A_1	τ_1 (s)	A_2	τ_2 (s)	R^2
Cr-MIL-101	0.54	0.6	0.43	29	0.963
Fe-MIL-101	0.36	0.8	0.63	54	0.976

2.2 Incorporation of capture probes into a Microfluidic Impedance Sensor Platform

To evaluate whether PFAS in drinking water is below the EPA thresholds, new sensing techniques for PFAS compounds in drinking water must be developed. Such sensors must be applicable for a spectrum of PFAS compounds that exist at very low concentrations. The sensors must also maintain their functionality when other substances with much higher concentrations are present. Current sensing technologies rely on ex situ laboratory techniques, such as liquid chromatography–mass spectrometry (LC-MS) and gas chromatography–mass spectrometry (GC-MS) [25-31]. However, the use of these methods in practical applications is restricted by their lack of adaption to on-site problems or their insufficient sensitivity to meet health advisory requirements.

We contributed to development of a detection technique incorporating our capture probes into an electrochemical platform designed primarily by NJIT using electrical impedance spectroscopy (Fig. 5A) [32]. The targeted capture of the PFAS induced an electrical response (increase in impedance). Further measures like optimization of the platform configuration and design and incorporation of additional, sensitive detection modalities have been undertaken to enhance the device sensitivity. Using this methodology, we have achieved detection limits as low as 0.5 ng/L for PFOS and 1.3 ng/L for PFOA. Although the measurements have notable imprecision, the apparent detection limits are significantly below the EPA health advisory level of 70 ng/L recommended by EPA.

The platform has potential for high sensitivity for a wide variety of PFAS concentrations and has shown promise in its ability to eliminate matrix interferences. Our demonstrated approach can detect multiple PFAS compounds in deionized water and groundwater as a matrix. In general, these sensors have the potential to enhance onsite quantification and remediation of PFAS contamination, in comparison to costly and difficult laboratory analysis techniques. By embedding the MOF capture probes in a microfluidic channel layered with interdigitated microelectrodes (IDμE), we were able to test the binding of PFOS to Cr-MIL-101 with electrochemical impedance spectroscopy (EIS). The sensing principle is based on the capture and binding of PFOS by Cr-MIL-101 leading to alteration of the charge transfer or polarization resistance due to change in the available electrode surface area.

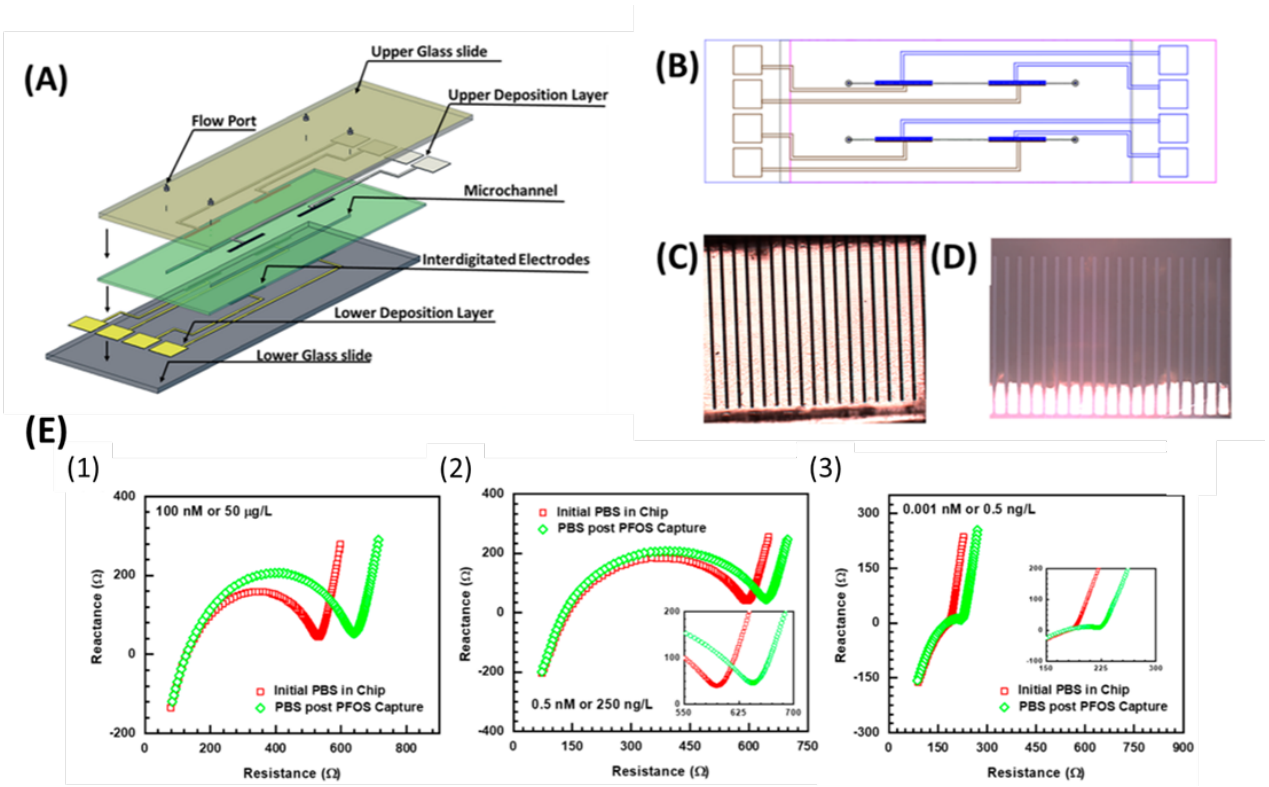

Fig. 5. (A) Schematics of the non-planar interdigitated chip used for PFOS detection with the microchannel cut from tape, filled with Cr-MIL101, and layered between two interdigitated microelectrode arrays (flow ports are indicated as well). (B) Top view of the assembled device. (C) Optical microscopic image of an empty microchannel (where MOF capture probe can be placed) with interdigitated electrodes. (D) Optical microscopic image of the microchannel with interdigitated electrodes filled with Cr-MIL-101. (E) Nyquist plot of the EIS response of the Cr-MIL-101 in 0.1X phosphate buffered saline buffer before and postexposure to (1) 50 µg/L PFOS, (2) 250 ng/L PFOS, and (3) 0.05 ng/L PFOS [32].

With all other circuit elements being chiefly parasitic and not contributing significantly to the resistance, we assume that this charge transfer or polarization resistance change is due to the binding of PFOS by Cr-MIL-101 is the key contributor to the sensor signal. The radius of curvature of the semicircular region in the Nyquist plot indicates that the charge transfer resistance increases in the Cr-MIL-101 post-PFOS exposure.

Table III. A comparison the limits of detection (LOD) for PFOS with our portable electrochemical technique relative to various state-of-the art laboratory-based *ex situ* techniques.

Technique	**LOD**
Liquid chromatography-tandem mass spectrometry (LC-MS/MS)	~1 ng/L
Time-of-flight mass spectrometry	1-10 ng/L
ex situ ion chromatography mass spectrometry	1-10 pg/L
Particle-induced gamma-ray	~10 nmol/cm^2
NMR	10 µg/L
TOP	1-10 ng/L
Our PNNL electrochemical technique	**Potentially 1 ng/L**

3.0 CONCLUSIONS

Our preliminary studies show improvement of technology development for both PFAS capture and separation, in terms of speed and capacity, relative to commercial sorbents (namely GAC). Additionally, the tunability of the nanoporous materials shows higher selectivity for the capture of the major representative PFAS from waste streams, groundwater, and industrial water. Ultimately, this technique is beneficial for the long-term removal of PFAS. Similarly, findings from our sensing work strongly suggest that our platform poses a promising approach for environmental monitoring. Further investigations about the transferability of our platform to other targets can be conducted in future work. We believe that this design can also be extended to other challenging emerging contaminants through modification and selection of appropriate receptor probes [9, 33]. The current EPS health advisory focus is on PFOS, or its carboxylate analog PFOA, but there are a total of ~6500 different PFAS molecules known. Recent studies indicate that the smaller chains can have higher toxicity (e.g., GenX). Our work has provided a proof-of-concept for PFOS detection and sensing at health advisory levels established by the EPA, along with capture/separation from water at elevated concentrations. This work provides a foundation for further development of materials for complete remediation of PFAS targets (such as GenX) by tailoring the capture probe.

4.0 References

(1) Hale, S. Reducing negative impact of PFAS https://www.ngi.no/eng/Projects/Reducing-negative-impact-of-PFAS/PFAS (accessed Nov 25, 2020).

(2) Per and Polyfluoroalkyl Substances (PFAS) | FDA https://www.fda.gov/food/chemicals/and-polyfluoroalkyl-substances-pfas (accessed Nov 25, 2020).

(3) Basic Information on PFAS | Per- and Polyfluoroalkyl Substances (PFAS) | US EPA https://www.epa.gov/pfas/basic-information-pfas (accessed Nov 25, 2020).

(4) Kucharzyk, K. H.; Darlington, R.; Benotti, M.; Deeb, R.; Hawley, E. Novel Treatment Technologies for PFAS Compounds: A Critical Review. J. Environ. Manage. 2017, 204, 757–764. https://doi.org/10.1016/j.jenvman.2017.08.016.

(5) Wu, C.; Klemes, M. J.; Trang, B.; Dichtel, W. R.; Helbling, D. E. Exploring the Factors That Influence the Adsorption of Anionic PFAS on Conventional and Emerging Adsorbents in Aquatic Matrices. Water Res. 2020, 182, 115950. https://doi.org/10.1016/j.watres.2020.115950.

(6) Chularueangaksorn, P.; Tanaka, S.; Fujii, S.; Kunacheva, C. Batch and Column Adsorption of Perfluorooctane Sulfonate on Anion Exchange Resins and Granular Activated Carbon. J. Appl. Polym. Sci. 2014, 131 (3). https://doi.org/10.1002/app.39782.

(7) Ochoa-Herrera, V.; Sierra-Alvarez, R. Removal of Perfluorinated Surfactants by Sorption onto Granular Activated Carbon, Zeolite and Sludge. Chemosphere 2008, 72 (10), 1588–1593. https://doi.org/10.1016/j.chemosphere.2008.04.029.

(8) Gebhardt, W.; Moreira, R. F. P. M.; Schro, H. F.; Jose, H. J.; Pinnekamp, J. Biological Wastewater Treatment Followed by Physicochemical Treatment for the Removal of Fluorinated Surfactants. 2010, 3208–3216. https://doi.org/10.2166/wst.2010.917.

(9) Barpaga, D.; Zheng, J.; Han, K. S.; Soltis, J. A.; Shutthanandan, V.; Basuray, S.; McGrail, B. P.; Chatterjee, S.; Motkuri, R. K. Probing the Sorption of Perfluorooctanesulfonate Using Mesoporous Metal-Organic Frameworks from Aqueous Solutions. Inorg. Chem. 2019, 58 (13), 8339–8346. https://doi.org/10.1021/acs.inorgchem.9b00380.

(10) Zheng, J.; Vemuri, R. S.; Estevez, L.; Koech, P. K.; Varga, T.; Camaioni, D. M.; Blake, T. A.; McGrail, B. P.; Motkuri, R. K. Pore-Engineered Metal-Organic Frameworks with Excellent Adsorption of Water and Fluorocarbon Refrigerant for Cooling Applications. J. Am. Chem. Soc. 2017, 139 (31), 10601–10604. https://doi.org/10.1021/jacs.7b04872.

(11) Zheng, J.; Barpaga, D.; Gutiérrez, O. Y.; Browning, N. D.; Mehdi, B. L.; Farha, O. K.; Lercher, J. A.; McGrail, B. P.; Motkuri, R. K. Exceptional Fluorocarbon Uptake with Mesoporous Metal-Organic Frameworks for Adsorption-Based Cooling Systems. ACS Appl. Energy Mater. 2018, 1 (11), 5853–5858. https://doi.org/10.1021/acsaem.8b01282.

(12) Zheng, J.; Barpaga, D.; Trump, B. A.; Shetty, M.; Fan, Y.; Bhattacharya, P.; Jenks, J. J.; Su, C. Y.; Brown, C. M.; Maurin, G.; McGrail, B. P.; Motkuri, R. K. Molecular Insight into Fluorocarbon Adsorption in Pore Expanded Metal-Organic Framework Analogs. J. Am. Chem. Soc. 2020, 142 (6), 3002–3012. https://doi.org/10.1021/jacs.9b11963.

(13) Motkuri, R. K.; Annapureddy, H. V. R.; Vijaykumar, M.; Schaef, H. T.; Martin, P. F.; McGrail, B. P.; Dang, L. X.; Krishna, R.; Thallapally, P. K. Fluorocarbon Adsorption in Hierarchical Porous Frameworks. Nat. Commun. 2014, 5, 1–6. https://doi.org/10.1038/ncomms5368.

(14) Barpaga, D.; Nguyen, V. T.; Medasani, B. K.; Chatterjee, S.; McGrail, B. P.; Motkuri, R. K.; Dang, L. X. Insight into Fluorocarbon Adsorption in Metal-Organic Frameworks via Experiments and Molecular Simulations. Sci. Rep. 2019, 9 (1), 1–10. https://doi.org/10.1038/s41598-019-46269-7.

(15) Jenks, J. J.; Motkuri, R. K.; TeGrotenhuis, W.; Paul, B. K.; McGrail, B. P. Simulation and Experimental Study of Metal Organic Frameworks Used in Adsorption Cooling. Heat Transf. Eng. 2017, 38 (14–15), 1305–1315. https://doi.org/10.1080/01457632.2016.1242965.

(16) Winarta, J.; Shan, B.; McIntyre, S. M.; Ye, L.; Wang, C.; Liu, J.; Mu, B. A Decade of UiO-66 Research: A Historic Review of Dynamic Structure, Synthesis Mechanisms, and Characterization Techniques of an Archetypal Metal-Organic Framework. Cryst. Growth Des. 2020, 20 (2), 1347–1362. https://doi.org/10.1021/acs.cgd.9b00955.

(17) Couck, S.; Denayer, J. F. M.; Baron, G. V.; Rémy, T.; Gascon, J.; Kapteijn, F. An Amine-Functionalized MIL-53 Metal-Organic Framework with Large Separation Power for CO2 and CH4. J. Am. Chem. Soc. 2009, 131 (18), 6326–6327. https://doi.org/10.1021/ja900555r.

(18) Ding, S. Y.; Wang, W. Covalent Organic Frameworks (COFs): From Design to Applications. Chem. Soc. Rev. 2013, 42 (2), 548–568. https://doi.org/10.1039/c2cs35072f.

(19) Lu, W.; Wei, Z.; Gu, Z. Y.; Liu, T. F.; Park, J.; Park, J.; Tian, J.; Zhang, M.; Zhang, Q.; Gentle, T.; Bosch, M.; Zhou, H. C. Tuning the Structure and Function of Metal-Organic Frameworks via Linker Design. Chem. Soc. Rev. 2014, 43 (16), 5561–5593. https://doi.org/10.1039/c4cs00003j.

(20) Fu, R. W.; Li, Z. H.; Liang, Y. R.; Li, F.; Xu, F.; Wu, D. C. Hierarchical Porous Carbons: Design, Preparation, and Performance in Energy Storage. Xinxing Tan Cailiao/New Carbon Mater. 2011, 26 (3), 171–179. https://doi.org/10.1016/S1872-5805(11)60074-7.

(21) Britt, D.; Furukawa, H.; Wang, B.; Glover, T. G.; Yaghi, O. M. Highly Efficient Separation of Carbon Dioxide by a Metal-Organic Framework Replete with Open Metal Sites. Proc. Natl. Acad. Sci. U. S. A. 2009, 106 (49), 20637–20640. https://doi.org/10.1073/pnas.0909718106.

(22) Mordenite Zeolite https://www.acsmaterial.com/blog-detail/mordenite-zeolite.html (accessed Nov 25, 2020).

(23) Gobelius, L.; Persson, C.; Wiberg, K.; Ahrens, L. Calibration and Application of Passive Sampling for Per- and Polyfluoroalkyl Substances in a Drinking Water Treatment Plant. J. Hazard. Mater. 2019, 362 (April 2018), 230–237. https://doi.org/10.1016/j.jhazmat.2018.09.005.

(24) Li, Y.; Yang, C.; Bao, Y.; Ma, X.; Lu, G.; Li, Y. Aquatic Passive Sampling of Perfluorinated Chemicals with Polar Organic Chemical Integrative Sampler and Environmental Factors Affecting Sampling Rate. Environ. Sci. Pollut. Res. 2016, 23 (16), 16096–16103. https://doi.org/10.1007/s11356-016-6791-1.

(25) Rodriguez, K. L.; Hwang, J. H.; Esfahani, A. R.; Sadmani, A. H. M. A.; Lee, W. H. Recent Developments of PFAS-Detecting Sensors and Future Direction: A Review. Micromachines 2020, 11 (7). https://doi.org/10.3390/mi11070667.

(26) Boulanger, B.; Vargo, J.; Schnoor, J. L.; Hornbuckle, K. C. Detection of Perfluorooctane Surfactants in Great Lakes Water. Environ. Sci. Technol. 2004, 38 (15), 4064–4070. https://doi.org/10.1021/es0496975.

(27) Taniyasu, S.; Kannan, K.; Man, K. S.; Gulkowska, A.; Sinclair, E.; Okazawa, T.; Yamashita, N. Analysis of Fluorotelomer Alcohols, Fluorotelomer Acids, and Short- and Long-Chain Perfluorinated Acids in Water and Biota. J. Chromatogr. A 2005, 1093 (1–2), 89–97. https://doi.org/10.1016/j.chroma.2005.07.053.

(28) Szostek, B.; Prickett, K. B.; Buck, R. C. Determination of Fluorotelomer Alcohols by Liquid Chromatography/Tandem Mass Spectrometry in Water. Rapid Commun. Mass Spectrom. 2006, 20 (19), 2837–2844. https://doi.org/10.1002/rcm.2667.

(29) Ylinen, M.; Peura, P. 'T'g'x Om, 9 1985. 1985, 717, 713–717.

(30) De Silva, A. O.; Mabury, S. A. Isolating Isomers of Perfluorocarboxylates in Polar Bears (Ursus Maritimus) from Two Geographical Locations. Environ. Sci. Technol. 2004, 38 (24), 6538–6545. https://doi.org/10.1021/es049296p.

(31) Alzaga, R.; Bayona, J. M. Determination of Perfluorocarboxylic Acids in Aqueous Matrices by Ion-Pair Solid-Phase Microextraction-in-Port Derivatization-Gas Chromatography-Negative Ion Chemical Ionization Mass Spectrometry. J. Chromatogr. A 2004, 1042 (1–2), 155–162. https://doi.org/10.1016/j.chroma.2004.05.015.

(32) Cheng, Y. H.; Barpaga, D.; Soltis, J. A.; Shutthanandan, V.; Kargupta, R.; Han, K. S.; McGrail, B. P.; Motkuri, R. K.; Basuray, S.; Chatterjee, S. Metal-Organic Framework-Based Microfluidic Impedance Sensor Platform for Ultrasensitive Detection of Perfluorooctanesulfonate. ACS Appl. Mater. Interfaces 2020, 12 (9), 10503–10514. https://doi.org/10.1021/acsami.9b22445.

(33) Chatterjee, S.; Norton, A. E.; Edwards, M. K.; Peterson, J. M.; Taylor, S. D.; Bryan, S. A.; Andersen, A.; Govind, N.; Albrecht-Schmitt, T. E.; Connick, W. B.; Levitskaia, T. G. Highly Selective Colorimetric and Luminescence Response of a Square-Planar Platinum(II) Terpyridyl Complex to Aqueous TcO4. Inorg. Chem. 2015, 54 (20), 9914–9923. https://doi.org/10.1021/acs.inorgchem.5b01664.

Pacific Northwest National Laboratory

902 Battelle Boulevard
P.O. Box 999
Richland, WA 99354

1-888-375-PNNL (7665)

www.pnnl.gov